

## SYNCHROTRON LIGHT INTERFEROMETRY AT JEFFERSON LAB\*

P. Chevtsov, A. Day, A.P. Freyberger<sup>†</sup>, R. Hicks  
 Jefferson Lab, 12000 Jefferson Avenue, Newport News VA 23606  
 J.-C. Denard  
 Synchrotron SOLEIL, 91192 CEDEX, France

### Abstract

The hypernuclear physics program at JLAB requires a tight upper limit on the RMS energy spread of  $\frac{\delta p}{p} < 3 \times 10^{-5}$ . The energy spread is determined by measuring the beam width at a dispersive location ( $D \sim 4\text{m}$ ) in the transport line to the experimental halls. Ignoring the  $\epsilon\beta$  contribution to the intrinsic beam size, this low energy spread corresponds to an upper bound on the beam width of  $\sigma_{beam} < 120\mu\text{m}$ . Typical techniques to measure and monitor the beam size are either invasive or do not have the resolution to measure the small beam sizes that correspond to such a small energy spread. These small beam sizes cannot be measured using direct focusing of the synchrotron or optical transition light due to diffraction limitations in the optics. Using interferometry of the synchrotron light produced in the dispersive bend, the resolution of the optical system can be made very small. The non-invasive nature of this measurement is also very advantageous as it allows continuous monitoring of the energy spread. Two synchrotron light interferometers have been built and installed at Jefferson Lab, one each in the Hall-A and Hall-C transport lines. The two devices operate over a beam current range from  $20\mu\text{A}$  to  $120\mu\text{A}$  and have a spatial resolution of  $10\mu\text{m}$ . The structure of the interferometer, the experience gained during its installation, beam measurements and energy spread stability are presented. Additionally, the dependence of the measured energy spread on beam current [bunch charge] will be presented.

### INTRODUCTION

The hypernuclear physics program at JLAB is attempting to measure very small mass splittings and widths of hypernuclear states. A 280 KeV mass resolution is needed for the experimenters to observe the closely spaced mass states. The mass of the hypernuclear state is measured by the “missing mass” technique, where the four vectors of the incoming and scattered electron are measured and used to determine the mass of the hypernuclear state. The equation for the missing mass squared, ( $M_X^2$ ) is:

$$M_X^2 = m_p^2 + 2m_p[E_0 - E'] + 2E_0E' \cos(\theta)$$

where  $E_0$  is the energy of the beam, and  $E'$  is the energy of the  $e^-$  after scattering off the proton target,  $m_p$ . Energy spread of the incident electron beam will broaden/smear

the  $M_X^2$  distribution. Of the 280 KeV resolution budget, 120 KeV is allocated to energy spread, which with  $E_0 = 4$  GeV results in a requirement of:

$$\frac{\sigma_E}{E_0} < 3 \times 10^{-5}.$$

This paper describes the instrumentation that has been installed in the end station transport beam-lines to measure and monitor the energy spread during these experiments.

### MEASURING ENERGY SPREAD

The transverse beam size,  $\sigma_{beam}$ , measured in a dispersive location has two sources:

$$\sigma_{beam} = \sqrt{\sigma_\beta^2 + \sigma_\delta^2},$$

where  $\sigma_\beta = \sqrt{\epsilon\beta}$  is the betatron size and  $\sigma_\delta$  is the size due to dispersion [1]. The energy spread is  $\frac{\sigma_E}{E_0} = \frac{\sigma_\delta}{D}$ , where  $D$  is the local dispersion. Ignoring the betatron contribution (which is safe to do when  $\frac{\sigma_\beta}{\sigma_\delta} \ll 1$ ) the upper limit on the energy spread is:

$$\frac{\sigma_E}{E_0} < \frac{\sigma_{beam}}{D}.$$

When the beam has a small energy spread, as with the JLAB beam,  $\sigma_\beta$  can be comparable to  $\sigma_\delta$  and the betatron contribution to the transverse beam size must be taken into account to determine the central value of the energy spread.

In order to minimize the betatron contribution to the beam size, as well as the effect of incoming dispersion, a special optics was devised for the end station transport line to increase the dispersion from 4 m (nominal) to 8 m (high dispersion).

In the JLAB transport lines the transverse beam size is measured by wire scanners, optical transition radiation monitors and synchrotron light interferometers. The operating ranges and capabilities of the devices are listed in Table 1. The devices have overlapping ranges which allows for cross calibration of the different devices. This paper describes the recently installed and commissioned synchrotron light interferometers in the A & C transport lines.

### SYNCHROTRON LIGHT INTERFEROMETER [SLI]

The use of synchrotron light interferometry makes it possible to measure the very small transverse beam size in a completely non-invasive manner [3, 4]. SLI installations

<sup>†</sup> freyberg@jlab.org

device	current range	beam interaction	measures
wire scanners/quad scan	$< 20\mu\text{A}$	invasive	$\sigma_E/E, \alpha, \beta, \gamma$
OTR [2]	$8 \rightarrow 180\mu\text{A}$	slightly invasive	$\sigma_{beam}$
SLI	$20 \rightarrow \infty\mu\text{A}$	non-invasive	$\sigma_{beam}$

Table 1: Tabulation of the operating range and capabilities of the three devices used to measure the transverse beam width in the end station transport lines.

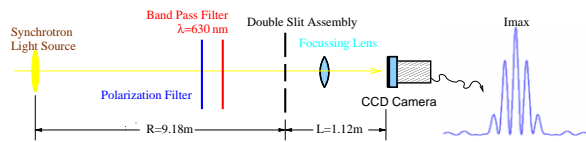


Figure 1: Cartoon schematic of the synchrotron light interferometer.

at storage rings have an abundant amount of synchrotron light due to the large stored beam current. The lower JLAB beam current is advantageous in that beam heating of the SLI optical components is no longer an issue as it is at storage rings. However, at these lower beam currents the intensity of the light is so diminished that a cooled CCD camera<sup>1</sup> is necessary to image the interferogram.

The difference in light intensity and the choice of CCD camera is the major difference between the JLAB SLI and that of T. Mitsuhashi at KEK [3, 4]. A sketch of the components used to make a SLI are shown in Figure 1 and details of the design are found in Ref. [5].

The beam size is a function of the visibility,  $\mathcal{V}$ , of the interference pattern:

$$\mathcal{V} = \frac{I_{max} - I_{min}}{I_{max} + I_{min}},$$

where  $I_{max}$  ( $I_{min}$ ) is the maximum (minimum) of the interference pattern. Since  $\mathcal{V}$  is a ratio, most systematics involved in digitization cancel. However, noise terms contribute to the sum [denominator] leading to a reduced  $\mathcal{V}$ , or larger calculated beam size and therefore must be kept small.

For a Gaussian beam distribution the beam size is found to be:

$$\sigma_{beam} = \frac{\lambda_0 R}{\pi d} \sqrt{0.5 \ln(1/\mathcal{V})},$$

where  $\lambda_0$  is the wavelength of the bandpass filter,  $R$  is the distance from the light source to the double slit assembly,  $d$  is the slit separation and  $\mathcal{V}$  is the measured visibility.

The JLAB SLI uses a grid pattern for the double slit assembly. This allows the simultaneous measurement of horizontal and vertical beam sizes. Figure 2 shows the real-time display of the interferogram data and fits to the data. The data update rate is a function of the beam current; as

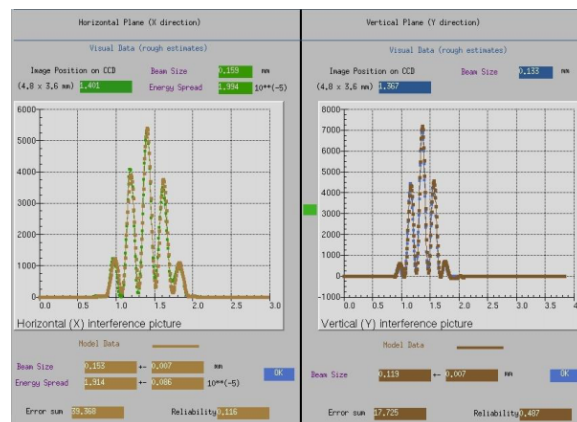


Figure 2: Control screen for the SLI showing the horizontal and vertical interferograms. The green (blue) points are the horizontal (vertical) data and the brown points are the result of a fit to the data. The values below the interferogram result from a fit to the expected functional form.

fast as 0.5 seconds for  $120\mu\text{A}$  and tens of seconds for beam currents less than  $20\mu\text{A}$ .

The video image is digitized and then analyzed. The analysis includes a simple first pass extraction  $I_{min}$  and  $I_{max}$ . These values are then used as the initial parameters for a non-linear least square fit of the data to the expected distribution. The free parameters in the fit are  $I_{min}$  and  $I_{max}$ . Once  $I_{min}$  and  $I_{max}$  are determined by the fit, the calculation of  $\mathcal{V}$  and the beam size is straight forward. In addition to the beam size, the quality of the fit,  $\chi^2$ , contains information on the alignment of the system as well as the validity of using a Gaussian distribution for the source term.

At the same location of the SLI there is an OTR monitor. Figure 3 is a plot of the beam sizes as measured by the OTR and SLI. There is a discrepancy with the larger beam sizes that is presently being investigated.

## OPERATIONAL EXPERIENCE

Figure 4 shows the stability of the energy for several days of operation. Initially the energy spread was near the specification of  $\frac{\sigma_E}{E} < 3 \times 10^{-5}$ . Improving the operation of the RF cavities and general machine setup resulted in a dramatic improvement of energy spread, seen on the plot as the drop in energy spread mid-day on April 23. The continuous operation of the SLI has proved to be useful in

<sup>1</sup>Santa Barbara Instrument Group, Astronomical CCD cameras, www.sbig.com.

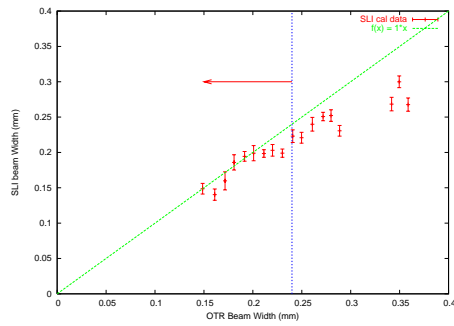


Figure 3: Plot of the beam width as measured by the SLI vs OTR. The green dashed curve is a line with slope of one and intercept of zero.

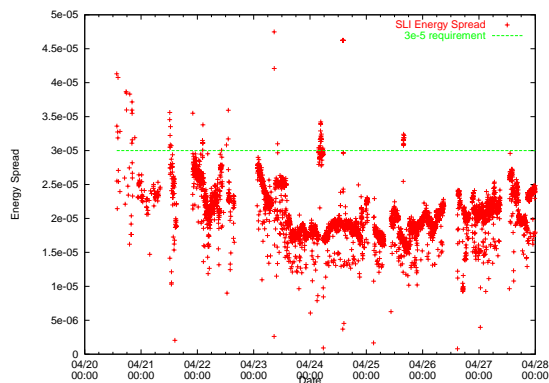


Figure 4: Plot of the SLI measurement of energy spread as a function of time for about a one week period. The experimental requirement of  $\sigma_E/E < 3 \times 10^{-5}$  is indicated by the green line.

identifying components contributing to the measured energy spread.

In addition to monitoring the energy spread during the experimental run, data was taken to study the energy spread as a function of the beam bunch charge. Simultaneous to the hypernuclear run in end-station A which used the JLAB nominal 499MHz beam structure, end-station C was receiving beam with a 31MHz beam structure. Both beams were delivered simultaneously and saw the same accelerating structures. The increase in energy spread with increasing bunch charge is expected due to space charge effects. Parmela simulations and measurements show an increasing longitudinal beam profile with bunch charge which results in a beam with an increased energy spread [6]. The energy spread requirement for the 31MHz beam of  $\sigma_E/E < 1 \times 10^{-4}$  was achieved simultaneously with the much tighter energy spread specification on the 499MHz beam.

## CONCLUSIONS

Instrumentation to measure and continuously monitor the energy spread at the end station transport lines has been presented. The end-station A SLI is fully commissioned

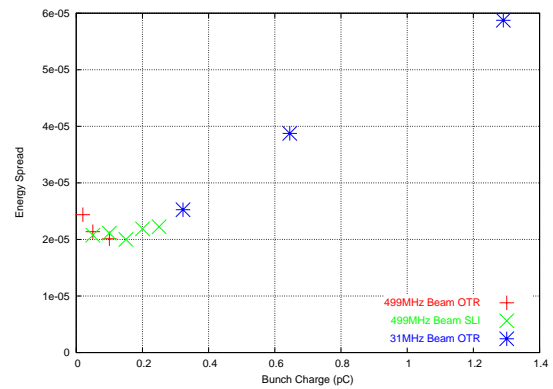


Figure 5: Plot of the energy spread as a function of the beam bunch charge. The JLAB nominal 499MHz and the novel 31MHz beam structures were used to obtain this data.

and contributed significantly to the recently completed hypernuclear experiment as well as to the understanding of the sources of energy spread degradation. The end-station C SLI is installed and being commissioned.<sup>2</sup> The hypernuclear experiment in end-station C runs mid-2005 and the SLI will be fully commissioned by then.

## ACKNOWLEDGMENTS

The authors thank the JLAB operations staff for support during commissioning the devices.

## REFERENCES

- [1] M.G. Minty and F. Zimmerman, *Measurement and Control of Charged Particle Beams*, Springer-Verlag, Berlin, 2003, pp. 163.
- [2] J-C. Denard *et al.*, “High Power Beam Profile Monitor with Optical Transition Radiation”, in *Proceedings of the 1997 PAC*, <http://accelconf.web.cern.ch/accelconf/pac97/papers/pdf/5P062.PDF>.
- [3] T. Mitsuhashi, “Beam Profile Measurement by SR Interferometers”, in *Proceedings of the Joint U.S.-CERN-Japan-Russia School on Particle Accelerators, Montreux, Switzerland, 1998*.
- [4] T. Mitsuhashi, “Faraday Cup Award Talk: 12 Years of SR Monitor Development at KEK”, in *Proceedings of the 2004 Beam Instrumentation Workshop*.
- [5] P. Chevtsov *et al.*, “Synchrotron Light Interferometer at Jefferson Lab”, in *Proceedings of the 2003 PAC*, <http://accelconf.web.cern.ch/accelconf/p03/PAPERS/WPPB068.PDF>.
- [6] Y. Zhang *et al.*, “A PAREMLA Model of the CEBAF Injector Valid Over a Wide Range of Parameters”, in *these proceedings*, paper TUPLT165.

<sup>2</sup>There are some alignment issues of the synchrotron source and the vacuum mirror that need to be fixed.